Wave Phenomena
Authors: Regis Zhao, Qingyuan Wu

April 16, 2021

INTRODUCTION

Waves are an omnipresent phenomena observed throughout our universe: sound, light, and vibrations of strings are just some examples of waves in everyday life. Waves' ubiquitous nature and diverse applications in science and engineering make them an extremely important topic of study. Many fundamental properties of waves can be observed by studying two-dimensional water waves. In this lab, we demonstrate laws and properties relevant to the reflection, wave speed, refraction, diffraction, and interference of waves. For reflection, we verify that for any reflective barrier, the angle of reflection is equal to the angle of incidence, i.e.:

$$\theta_i = \theta_r \tag{1}$$

Wave speed, or the rate at which waves propagate, is a function of multiple variables, including the wavelength, frequency, and depth of water for water waves. These can be summarized into two equations, which we will verify:

$$v = \lambda f \text{ and } v = \sqrt{gd} \tag{2) and (3}$$

where v is the wave speed, λ is the wavelength, f is the wave frequency, g is the acceleration due to gravity, and d is the depth of the water. Refraction occurs when a travelling wave crosses into another medium with a different speed of propagation. This results in the wave appearing to bend after entering the new medium, i.e. the angle of refraction differs from the angle of incidence. The relationship between these angles and media are examined using the relationship:

$$\frac{1}{v_1}\sin \theta_1 = \frac{1}{v_2}\sin \theta_2 \tag{4}$$

where the subscripts 1 and 2 denote the two different media, v is the velocity at each medium, and θ is the angle between the wavefronts and the normal to the surface boundary. Diffraction is another important physical phenomena observed in waves, occurring when passing around objects or barriers. A common method of observing this is propagating a wave through a slit. Properties of diffraction can be understood using the equation:

$$a \sin \theta = \lambda \tag{5}$$

where a is the width of the opening and θ is the angular spread. Finally, we investigate the interference of two coherent waves whose sources are a small distance apart. The amplitude of the superposition of the two waves is equal to zero along lines where the distance travelled by the two interfering waves is a whole number multiple of the wavelength. These points satisfy the following relation:

$$d \sin \theta_m = m\lambda, \, m = 1, 2, 3... \tag{6}$$

where d is the separation distance between the two sources, θ_m is the angle of deviation, and m is an integer representing the order of the interference. The condition under which (6) is satisfied is known as destructive interference between two coherent waves. At lines of destructive interference the wave amplitude is zero. This is clearly noticeable in the case of a water wave as lines that do not ripple over time signify destructive interference. We use a ripple tank filled with water, a ripple generator, different types of barriers, as well as an image acquisition software called "Ripple Tank" to generate the different wave patterns and obtain data. The purpose of this lab is to experimentally verify the aforementioned properties and mathematical relations of two-dimensional waves using this ripple tank.

MATERIALS AND METHOD
Materials
- Ripple tank filled with water
- Ripple generator; frequency uncertainty of $\pm\ 0.05\ Hz$
- Light source
- Dippers, shown in Figure 1
- Barriers, shown in Figure 1
- "Ripple Tank" image acquisition software (also used for length measurements; uncertainty of $\pm\ 0.005\ cm$)
- Ruler; uncertainty of $\pm\ 0.05\ cm$
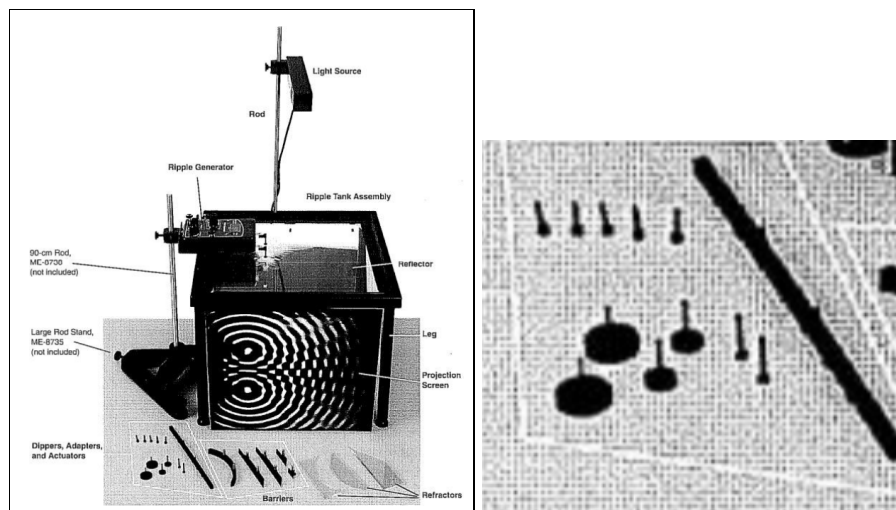- Protractor; uncertainty of $\pm\ 0.5^{\circ}$

Figure 1. (left) Experimental setup. (right) The long, straight rectangular object is the plane wave dipper. The two medium-sized cylinders are the standard dippers.

Methods
The ripple generator was used to create water waves at variable frequencies and amplitudes. The plane wave dipper (which generated plane waves) was used for all parts of the experiment except

for the interference portion, where two standard dippers were used instead to generate waves from two sources. Images of wave patterns of this experiment were obtained using the "Ripple Tank" image acquisition tool. Whenever wavelength was measured, five measurements were made and the average of those was taken and used as the value for wavelength. Wavelengths were measured using the measuring tool provided in the "Ripple Tank" software. The phase switch on the ripple generator was set to be in phase for the entirety of the lab except for the last portion of the interference component, where the interference pattern of out-of-phase waves was investigated.

Reflection

Reflection was studied using a straight barrier as well as a curved one. The long straight barrier was first placed at an angle in the middle of the tank. The frequency of the ripple generator was set to 20 Hz. Measurements of the incidence and reflection angles were taken using a protractor. The straight barrier was then replaced with the curved barrier. It was first placed such that it curved towards the ripple generator. The focal distance and radius of the curved distance were estimated. This process was then repeated with the curved barrier flipped 180 degrees, i.e. curving away from the ripple generator

Wave Speed

Wave speed was studied in two ways: with varying wave frequency and varying water depth. All barriers were removed from the tank. For varying wave frequency, the wavelength was first measured with five varying wave frequencies by starting the ripple generator at 5 Hz and increasing by 5 Hz each time to 25 Hz. For varying water depths, the frequency of the ripple generator was fixed at 10 Hz while the height of the ripple generator was adjusted for five different trials such that the waves generated occurred at the following depths: 1mm, 2mm, 3mm, 4mm, and 5mm.

Refraction

The trapezoidal refractor was placed in the middle of the tank with the triangular side pointing towards the ripple generator. The water level was adjusted such that it was roughly 2 mm above the surface of the refractor. The ripple generator was set to a 15 Hz frequency and the angles of incidence and refraction were measured.

Diffraction

Two straight barriers were placed in the tank facing the ripple generator to create a slit. The ripple generator was set to a frequency of 20 Hz. The angular spread of the wave pattern was measured using a protractor for four different trials, where the size of the slit (distance between the barriers) was adjusted from 2.5 cm to 4 cm, incrementing by 0.5 cm each trial. The angular spread was measured as the angle between the line perpendicular to the wavefronts and the line outlining the diffraction of the wavefronts.

Interference

The standard dippers attached to the ripple generator were set at 2.6 cm apart and the frequency was set to 20 Hz. Observing the resulting wave pattern, the angles formed between the lines joining the first and second orders of destructive interference were measured using a protractor. The wavelength was also measured. The same measurements were performed for 3 more trials with varying distances between the dippers: 5.1 cm, 7.7 cm, and 10.25 cm. The method for this portion of the lab was then repeated with the dippers set out of phase with each other by flipping the phase switch.

DATA AND ANALYSIS
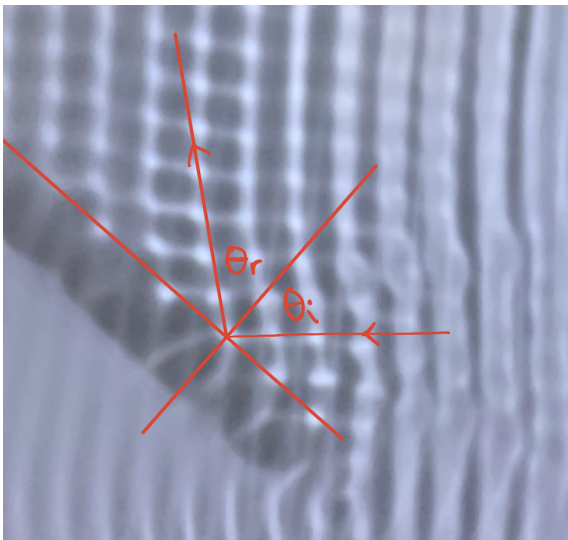
1. Reflection

1.1 Straight Barrier

Figure 2. Wave reflection pattern generated with a straight barrier placed at an angle in the tank. θ_i is angle of incidence; θ_r is the angle of reflection.

Red lines are drawn to serve as a visual aid for the plane of the barrier, the normal, and incident and reflected waves. As measured from a protractor, $\theta_i = 49° \pm 0.5°$,

$\theta_r = 51° \pm 0.5°$. Although these values do not mutually lie within each other's uncertainties, they are consistent with 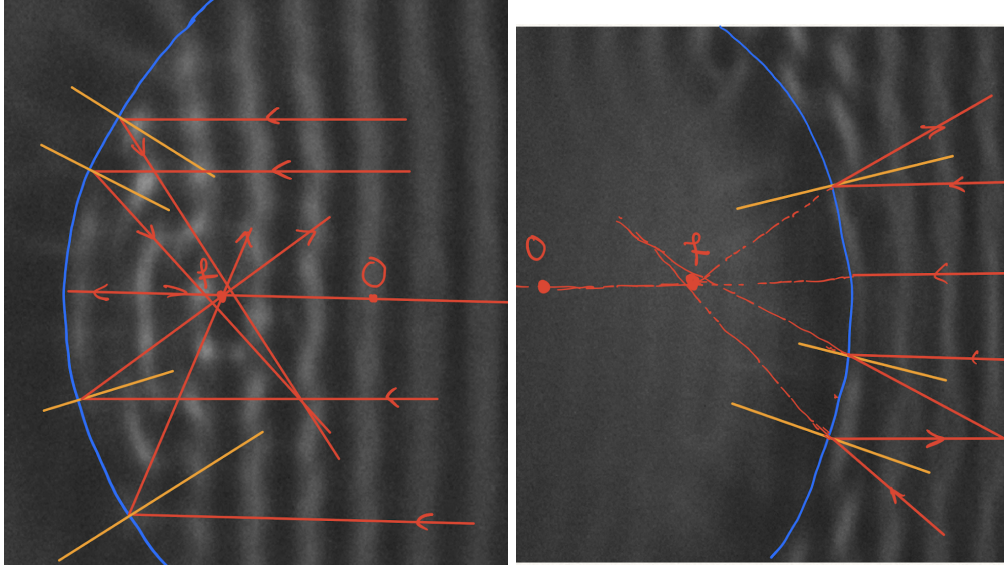each other as their uncertainties do overlap. Therefore Equation 1 provides us with a valid equation modelling the relationship between the incidence and reflection angle. Other than the measurement limitations of the protractor, another major source of uncertainty is the drawing of incident and reflected waves that accurately represent the behaviour of the actual water waves. Upon careful examination of Fig. 2, one can see that the water waves change angles slightly upon approaching the barrier. This increases the error potential of the hand-drawn incident and reflected waves, and thus the calculation of θ_i and θ_r.

1.2 Curved Barriers

Waves reflect off of the curved barrier according to the same law, $\theta_i = \theta_r$. However, due to a curved surface, it is important to draw the normal, from which the angles are measured,

perpendicular to the tangent to the surface at the point of contact. The wavelength was measured to serve as a scale when approximating the focal length.

$$\lambda = 1.07 \ cm$$

Bending **towards** Source	Bending **away from** Source
Figure 3a (left) 3b (right). Wave reflection pattern generated with curved barrier placed curving towards (left) and away from (right) the ripple generator. f is the focal point; O is the center of the circle created by the curved barrier. The blue curve outlines the position and shape of the barrier closest to the incident waves. The red lines are samples of incident and reflected water waves. These waves reflect according to $\theta_i = \theta_r$. The orange lines are normal to the curved surface. They are drawn for verification that the incident and reflected angles are equal.	
The focal distance, L, is measured as the approximate number of wavelengths that the curved surface is from the focal point. The radius of curvature, R, is exactly twice the length of the focal distance [1].	
$L = 3.21 \pm 0.3 \ cm$ The focal distance was approximately 3.0 ± 0.1 wavelengths away from the barrier.	$L = 3.42 \pm 0.3 \ cm$ The focal distance was approximately 3.2 ± 0.1 wavelengths away from the barrier.
$R = 2L = 6.42 \pm 0.3 \ cm$	$R = 2L = 6.84 \pm 0.3 \ cm$

2. Wave Speed

2.1 Wave Speed and Frequency

Wave speed is only dependent on the properties of its medium[3]. Therefore, by rearranging Equation 2, we can see that a given medium's wave speed should be constant and we should observe an inverse relationship between the frequency and wavelength

$$\lambda = v/f \tag{7}$$

Below (Figure 4) is a graph of wavelength plotted against frequency, where the properties of the medium (i.e. the water in the ripple tank) remained constant. We can see that, as expected, we observe an inverse relationship between the two variables; the wavelength decreases as frequency increases and vice versa. By fitting the data to the function described by Equation 7 we obtain an approximation for v, the wave speed of the medium, to be $20.8954\ cm/s$. This velocity does not have an associated uncertainty since it was produced by the computer program after generating the curve of best fit shown in Figure 4.
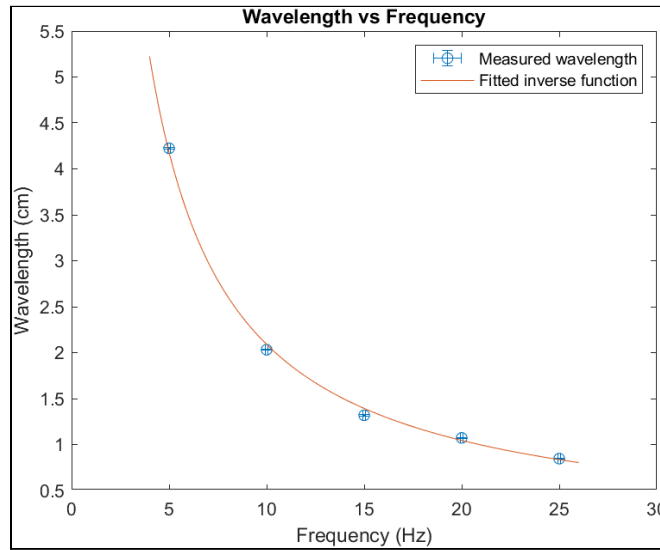
Figure 4. Measured wavelength plotted against frequency. The data is fitted to the function $\lambda = v/f$, where $v = 20.8954\ cm/s$. Uncertainty in wavelength: ±0.005 cm; uncertainty in frequency: ±0.05 Hz (error bars are too small to be seen in the graph).

The reduced χ^2 of the fitted function was calculated to be 1.18. Since this value is close to 1, the function is a good fit for the data, though the uncertainties of the measured wavelengths still may be slightly too small since $1.18 > 1$. Looking at the residuals of the fitted function, there does not seem to be any obvious trends or patterns, which also supports that the fit of the function is a good one.

Equation 2 was also used to calculate the wave speed for the five trials of varying frequencies. The average calculated wave speed for the medium was calculated to be $20.76 \pm 0.25\ cm/s$. Comparing the approximation of the wave speed obtained from the fitted function to this calculated value, v obtained from the fitted function lies within the uncertainty of the value of v calculated using Equation 2. Therefore, Equation 2 serves as a good model for the relationship

between wave speed, frequency, and wavelength. Sources of error that could have affected the results include the instrumental uncertainties of the "Ripple Tank" software and ripple generator.

2.2 Wave Speed and Water Depth

Per Equation 3, wave speed is proportional to the square root of the water depth, where the constant of proportionality is the square root of Earth's gravitational constant, 9.81 m/s². Wave speed was calculated by measuring the wavelengths and using Equation 2. Below is a graph of wave speed plotted against the water depth, fitted to the function described by Equation 3. The fitted function approximates the value of g to be 981.21 cm/s², or equivalently, 9.8121 m/s². This is extremely close to the true value of Earth's gravitational constant, supporting the validity of Equation 3.
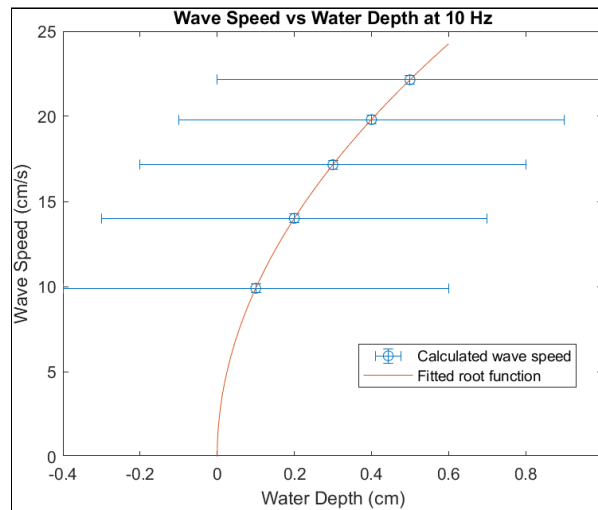

Figure 5. Calculated wave speed plotted against water depth. The data is fitted to the function
$v = \sqrt{gd}$, *where g is approximated to be 981.21 cm/s².*

The reduced χ^2 of the fitted function was calculated to be 0.0002. Since this value is much smaller than the ideal value of 1, the data has likely been overfitted and therefore the function may not be a good fit for the data. However, the residuals of the fitted function showed no obvious trend, which is evidence the fit of the function is a good one.

There are numerous sources of error that could have affected the data, including the instrumental uncertainty of the "Ripple Tank" software and ripple generator mentioned before, as well as the instrumental uncertainty of the ruler used to measure water depth.

3. Refraction

As discussed in the introduction, refraction occurs when waves cross into a medium with a different speed of propagation. As we saw in the previous section, water depth affects wave speed. Therefore, by placing the trapezoidal refractor in the tank, we create an area where the

water depth is significantly shallower than its surroundings, resulting in a different wave propagation speed, thus causing refraction.
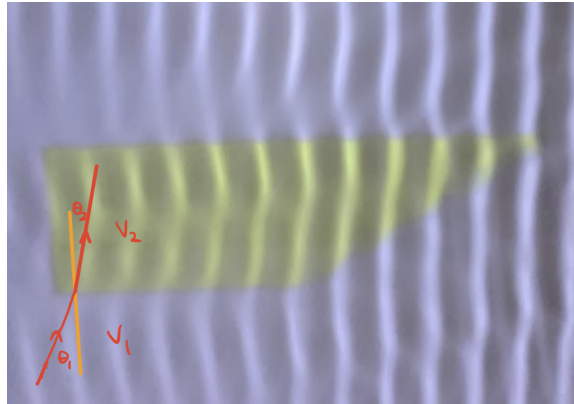

Figure 6. The refraction of water waves due to the change in depth in the trapezoidal refractor's medium.

The objective of this portion of the lab is to verify the law of refraction, given by Equation 4, given by $\frac{1}{v_1}\sin\theta_1 = \frac{1}{v_2}\sin\theta_2$. We use the subscript 1 for all values in the tank regime, 2 for all values in the refractor's regime. Therefore, θ_1 is the angle between the incident wave and the normal, θ_2 is the angle between the refracted wave and the normal, v_1 is the incident wave velocity, and v_2 is the refracted wave velocity. These values are summarized in Table 1 below.

(Table 1) Measured and calculated values for wave properties in the tank and refractor media.

	Tank, 1	Refractor, 2
Depth	$d_1 = 5 \pm 0.5\ mm$	$d_2 = 2 \pm 0.5\ mm$
Speed	$v_1 = 22.15 \pm 0.25\ cm/s$	$v_2 = 14.01 \pm 0.25\ cm/s$
Angle	$\theta_1 = 28° \pm 0.5°$	$\theta_2 = 17° \pm 0.5°$
$(\sin\theta)/v$	$0.0212 \pm 0.0004\ s/m$	$0.0209 \pm 0.0007 s/m$

The last row of Table 1 represents the left and right sides of Equation 4. These values, in theory, should be equal. While the calculated values are not exactly equal, they both lie within each other's uncertainties and therefore agree with each other, verifying the law of refraction (Equation 4).

4. Diffraction

As discussed in the *Wave Speed* section, the wave speed of a medium with unchanging properties will also be constant. In this part of the lab, the frequency of the ripple generator was also
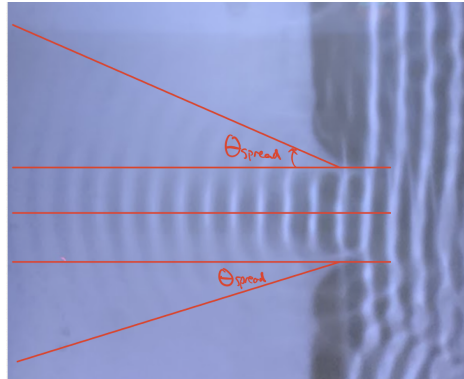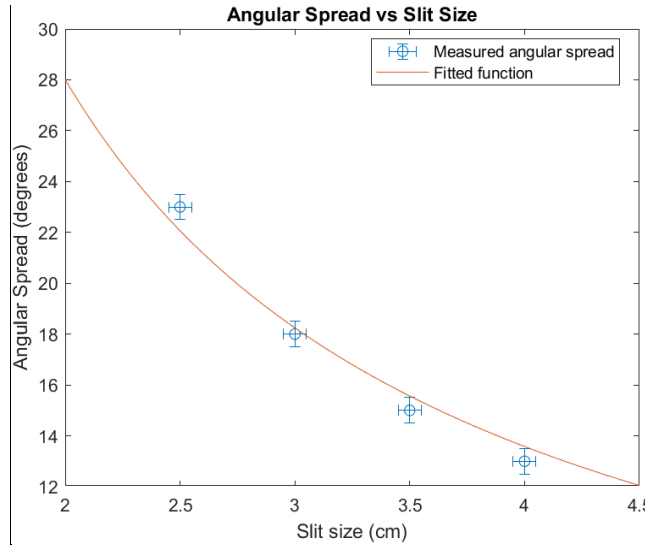

Figure 7. Diffraction wave pattern created by placing two barriers to create a slit opening. Angular spread θ_{spread} is labelled.

held constant at 20 Hz, therefore, the wavelength theoretically should also have remained constant. The wavelength was measured to be 1.01 cm +/- 0.005 cm. As we can see from Equation 5, for a constant wavelength, there exists an inverse relationship between *a* and theta since $\sin \theta$ monotonically increases for $\theta \in [0^{\circ}, 90^{\circ}]$. Therefore, the smaller the slit opening, the larger the angular spread and vice versa. Below is a graph plotting the measured angular spread against the slit size opening. Rearranging Equation 5 for theta, we obtain:

$$\theta = \arcsin (\lambda/a) \tag{8}$$

providing us with a function to fit the data to. The fitted function approximates the wavelength lambda to be $0.9392\ cm$. While this value is close to the measured wavelength, it does not lie within the measured wavelength's uncertainty. These values therefore do not agree with each other and Equation 5 cannot be verified by looking at the wavelength approximation alone - by judging the fitted function below, Equation 5 still serves as a valid model for the relationship between the angular spread and slit size.

(Figure 8) Angular spread plotted against slit size. The data is fitted to the function
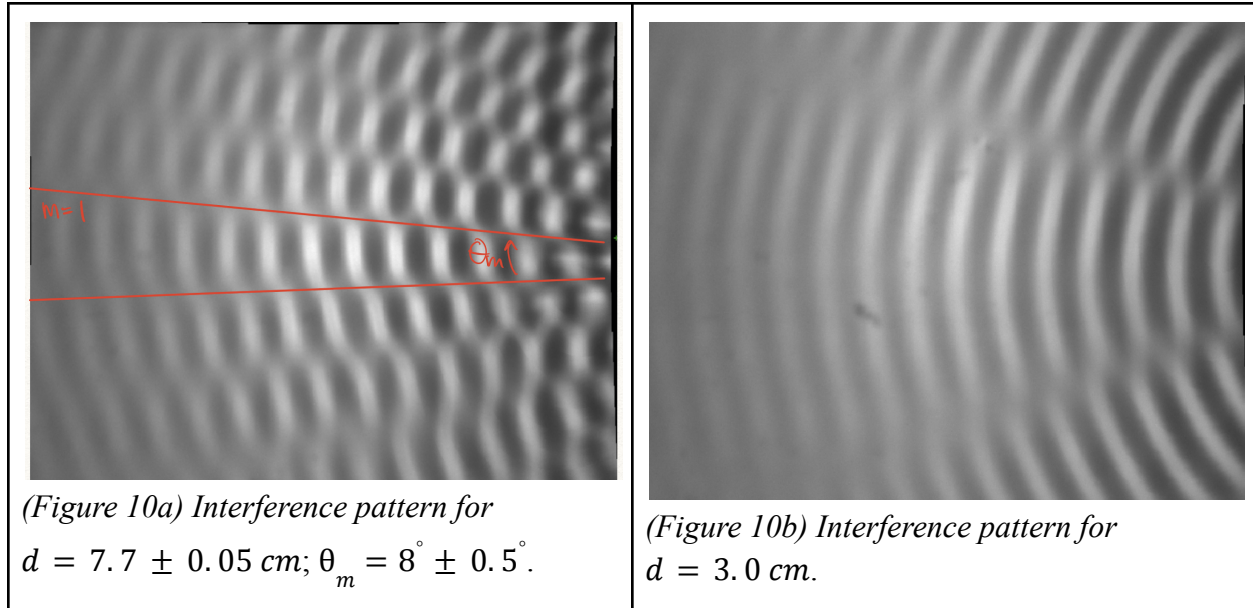$$\theta = \arcsin(\lambda/a), \text{ where } \lambda = 0.9392 \pm.... \ cm.$$

The reduced χ^2 of the fitted function was calculated to be 18.66, which is much larger than the ideal value of 1. This indicates that the uncertainties of the angular spread are likely too small, implying that the fitting function might not be a good fit for the data. Looking at the residuals of the fitted function, they once again show no obvious trend, supporting that the fit of the function is a good one.

Sources of error that could have affected these results include the instrumental uncertainties of the "Ripple Tank" software when measuring the wavelength, ruler when measuring the slit size, and protractor when measuring the angular spread.

5. Interference

<u>5.1 In-Phase Vibrations</u>
Recall the interference equation: $d\sin(\theta_m) = m\lambda, \ m = 1, 2, 3...$ (6). This equation is obeyed by all points at which there is destructive interference. In plain words, Equation 6 asserts that interference occurs when the waves from one of the sources travel exactly a whole number multiple wavelengths of extra distance compared to the waves from the other source. For convenience, m was chosen to be 1, representing the first order of interference. θ was therefore measured as the angle between the two lines of destructive interference, shown in red in Figure 10, closest to the normal. Five wavelength measurements were taken and the average between them was used as the final wavelength.

(Figure 10a) Interference pattern for $d = 7.7 \pm 0.05\ cm$; $\theta_m = 8° \pm 0.5°$.

(Figure 10b) Interference pattern for $d = 3.0\ cm$.

(Table 3) Comparing interference patterns with different slit distances, d.

Using the Equation 6 with $m = 1$ and solving for d, we get d =

$\lambda/\sin\theta_1 = 1.112/\sin(8°) = 7.99\ cm$. This agrees within 4% with the actual, measured value for the slit distance, $7.7 \pm 0.05\ cm$. The interference pattern changes as a function of the slit distance d. As d increases the angle between consecutive points of constructive/destructive interference decreases according to Equation 6, so the interference pattern "shrinks" - there is a smaller distance between consecutive constructive/destructive points. Comparing Figure 10a and 10b, with $d = 7.7 cm$, the distance between consecutive points of zero amplitude (destructive) greatly increased. Here, θ_b is around 30 degrees compared to θ_a which was less than 10 degrees.

Finally, note that Equation 6 itself is an approximation that must operate under the assumptions that the point is far away from the wave sources. Other geometric approximations were also used to arrive at the equation.

5.2 Out-of-Phase Vibrations

Now dippers were set to vibrate out of phase. This meant that the light sources were incoherent - they were produced at different frequencies. The interference pattern was thus fluctuating and time-variant. This is in contrast to the interference patterns of two in-phase sources which remained constant through time. For out-of-phase wave sources, the wave interference equation can be reformulated as follows:

$\psi(x_p, y_p, t) = A_0 \cos(w(t - \frac{r_1}{v})) - A_0 \cos(w(t - \frac{r_2}{v})) = -2A_0 \sin(\omega t) \sin(\frac{\pi(r_2 - r_2)}{\lambda})$. This can be compared with the original wave amplitude equation for in-phase sources:

$$\psi(x_p, y_p, t) = A_0 \cos(w(t - \tfrac{r_1}{v})) + A_0 \cos(w(t - \tfrac{r_2}{v})) = 2A_0 \cos(\omega t) \cos(\tfrac{\pi(r_2 - r_2)}{\lambda})$$

We simply changed the sign of the second cosine term since the waves are out of phase now.

MAJOR SOURCES OF UNCERTAINTIES

These uncertainties had a relatively significant impact on the results, and applied to most or all components of the lab.

- Inconsistency between the computer-measured wavelength and the actual wavelength. This source of error is a recurring theme throughout the experiments since many computer-aided measurements were made. This will be further discussed as a potential for improvement in the *Conclusion* section.
- Hand measurement of angle measurements had relatively large uncertainties due to the limitations of the protractor
- The lighting and pixelization of the image capturing tool can be improved.

ERROR ANALYSIS

All uncertainties for calculated values were calculated using the following formulas for error propagation. For multiplication and division operations:

$$\sigma_f = f\sqrt{(\tfrac{\sigma_a}{a})^2 + (\tfrac{\sigma_b}{b})^2 + \ldots} \tag{9}$$

where σ_x is the uncertainty in variable x, and f, the computed result, is a function of variables a, b, etc. For addition and subtraction operations:

$$\Delta z = \sqrt{(\Delta x)^2 + (\Delta y)^2 + \ldots} \tag{10}$$

where Δx, Δy are the uncertainties for the variables x, y.

CONCLUSION

This report detailed the demonstration of six wave phenomena equations, namely equations for reflection, wave speed's dependence on frequency and water depth, refraction, diffraction, and interference. 2D water waves generated by a plane wave dipper were the source of measurements used to confirm or reject these equations. Interestingly, with the exception of wave speed's dependence on water depth (Equation 3), all other equations apply to waves in general, such as electromagnetic and sound waves. All equations, except Equation 5, were verified as any deviations existed within uncertainties. However, large experimental uncertainties reduced the credibility of these verifications. In the future, uncertainties should be reduced through (1) better image acquisition techniques, which would make drawing lines for angle measurements much more accurate; (2) more accurate length determination tools. Currently, the measurement tool supplied by the software Ripple Tank differed slightly from measurements by a ruler.

APPENDIX

Raw Data

Table A1. Wave speed and frequency - raw data.

$f\,(Hz)$	$\lambda_1(cm)$	$\lambda_2(cm)$	$\lambda_3(cm)$	$\lambda_4(cm)$	$\lambda_5(cm)$	$\lambda_{ave}(cm)$	Standard deviation, $\sigma\,(cm)$	Velocity, $v\,(cm/s)$
5	4.2	4.22	4.34	4.14	4.22	4.224	0.072664	21.12
10	1.94	2.03	2.05	2.11	2.03	2.032	0.060992	20.32
15	1.3	1.34	1.35	1.32	1.28	1.318	0.028636	19.77
20	1.1	1.08	1.04	1.06	1.08	1.072	0.022804	21.44
25	0.85	0.85	0.83	0.87	0.83	0.846	0.016733	21.15

Table A2. Wave speed and water depth - raw data.

depth (mm)	$\lambda_1\,(cm)$	$\lambda_2\,(cm)$	$\lambda_3\,(cm)$	$\lambda_4\,(cm)$	$\lambda_5\,(cm)$	$\lambda_{ave}\,(cm)$	Standard deviation, $\sigma\,(cm)$	Velocity, $v\,(cm/s)$
5	2.13	1.97	1.97	2.03	2.15	2.05	0.086023	22.14723
4	2.19	2.07	1.99	2.19	2.07	2.102	0.086718	19.80909
3	2.09	2.07	2.11	2.13	2.01	2.082	0.046043	17.15517
2	2.11	2.07	2.11	2.09	2.13	2.102	0.022804	14.00714
1	2.05	2.07	2.09	2.13	2.09	2.086	0.029665	9.904544

$\lambda_1 - \lambda_5$ for the above two tables are five separate wavelength measurements. λ_{ave} and σare calculated based on these five measurements.

Table A3. Diffraction - raw data

slit length	2.5	3	3.5	4
angular spread	23	18	15	13
expected angular spread	23.8	19.7	16.8	14.6

The diffraction patterns at various opening sizes. All θ_{actual} uncertainties are $\pm\,0.5°$; all a uncertainties are $\pm\,0.05cm$.

Table A4. Interference - raw data

Slit distance, $d\,(cm)$	$\lambda_1(cm)$	$\lambda_2(cm)$	$\lambda_3(cm)$	$\lambda_4(cm)$	$\lambda_5(cm)$	$\lambda_{ave}\,(cm)$
2.6	1.12	1.08	1.06	1.14	1.1	1.1

5.1	1.1	1.06	1.06	1.08	1.14	1.088
7.7	1.1	1.12	1.08	1.12	1.14	1.112
10.25	1.18	1.16	1.14	1.18	1.18	1.168

$\lambda_1 - \lambda_5$ are five separate wavelength measurements. λ_{ave} is the average of these measurements.

REFERENCES

[1] https://physics.info/mirrors/

[2] Lab Manual: Wave Phenomena

[3] https://www.physicsclassroom.com/class/waves/Lesson-2/The-Speed-of-a-Wave